Eur. Phys. J. D **46**, 51–57 (2008)
DOI: 10.1140/epjd/e2007-00278-2

THE EUROPEAN PHYSICAL JOURNAL D

Influence of pressure on the relative population of the two lowest vibrational levels of the C $^3\Pi_u$ state of nitrogen for electron beam excitation

A. Morozov[1,a], T. Heindl[1], J. Wieser[2], R. Krücken[1], and A. Ulrich[1]

[1] Physik Department E12, Technische Universität München, 85748 Garching, Germany
[2] Coherent GmbH, Zielstattstrasse 32, 81379 München, Germany

Received 14 June 2007 / Received in final form 4 September 2007
Published online 28 September 2007 –

Abstract. Continuous and pulsed 12 keV electron beams were used to excite nitrogen within a gas cell at pressures ranging from 10 to 1400 hPa. The pressure dependence of the ratio of photon fluxes for emission from vibrational levels $v' = 0$ and 1 of the C $^3\Pi_u$ state has been studied. The results confirm the presence of a collisional excitation mechanism populating $v' = 0$, 1 in addition to electron impact excitation. Rate constants of $(1.27 \pm 0.04) \times 10^{-11}$ cm^{3}s^{-1} $[v' = 0]$ and $(2.68 \pm 0.08) \times 10^{-11}$ cm^{3}s^{-1} $[v' = 1]$ were measured for C $^3\Pi_u$ quenching by ground state nitrogen. For electron beam conditions relative excitation efficiencies of 1:0.59:0.22 for vibrational levels 0, 1 and 2 were calculated. The recorded flux ratios are compared with the predictions given by a vibrational relaxation model.

PACS. 34.80.Gs Molecular excitation and ionization by electron impact – 33.70.Fd Absolute and relative line and band intensities – 33.50.Hv Radiationless transitions, quenching

1 Introduction

Excitation of molecular nitrogen by electron beams or electrical discharges leads to strong light emission from N_2 C $^3\Pi_u \rightarrow$ B $^3\Pi_g$ transitions, the so-called second positive system (SPS). Since this emission appears practically at all gas densities and its wavelength lies in an easily accessible range with the most intense bands between 300 and 400 nm, SPS emission is often used to obtain information on gas temperature (e.g. [1]), gas kinetics (e.g. [2,3]) or to monitor parameters of the excitation [4].

Radiative lifetimes as well as rate constants of collisional quenching by ground state nitrogen have been investigated for the lowest vibrational levels of the C $^3\Pi_u$ state in a significant number of studies (e.g. [5–12]). However, excitation mechanisms which populate the vibrational levels of the C $^3\Pi_u$ state from other electronic states of N_2 (or other vibrational levels of the C $^3\Pi_u$ state) due to collisions with ground state molecular nitrogen received much less attention. In 1971, Calo and Axtmann [10] have claimed the existence of vibrational relaxation within the C $^3\Pi_u$ state due to collisions with ground state N_2. Recently, two more papers were published. Panchesnyi et al. [6] state that vibrational relaxation is weak analysing their time-resolved results from pulsed discharge excitation. In contrast, Dilecce et al. [5] give a table of vibrational relaxation rate constants with significant values derived from a combination of dielectric barrier discharge and laser induced fluorescence. Also, some studies have indicated [13,14] a possible contribution of the E $^3\Sigma_g^+$ state to the population of the C $^3\Pi_u$ state in collision-induced channels.

In this paper, we confirm that for electron beam excitation of dense gases there is at least one excitation mechanisms which populates the lowest vibrational level of the C $^3\Pi_u$ state in addition to electron impact excitation. This conclusion is based on measurements of the pressure dependence (10–1400 hPa) of the ratio of photon fluxes for vibrational levels 0 and 1 and on time resolved observations of the SPS emission. We also present new values for quenching rate constants for nitrogen in the two lowest vibrational levels of the C $^3\Pi_u$ state which are relevant for an analysis of the photon flux data. The results presented in this paper suggest significant modification of the model in the studies of fluorescence emission from the C $^3\Pi_u$ state in dense nitrogen and air reported e.g. in references [4,15–17] where the electron impact excitation of the C $^3\Pi_u$ state is considered to be the only excitation channel.

2 Experimental details

Excitation of nitrogen was performed with electron beams. A detailed description of the method has been presented

[a] e-mail: andrei.morozov@ph.tum.de

in [3]. In short, a 12 keV electron beam from an electron gun was sent through a ∼300 nm thick silicon nitride foil into gas. Target gas pressures ranged from 10 to 1400 hPa. The gas cell was a 22 mm long stainless steel cylinder with an inner diameter of 35 mm. The target gas was continuously circulated through the cell and a buffer volume with a metal bellows compressor. The cell had a MgF_2 window. The inner walls were covered with a thin layer of gold to minimize impurity production during operation. Nitrogen with a purity of 99.9999% was used. Light output was resolved with a McPherson monochromator (Model 218) and detected either with a photo-multiplier tube (S20 cathode) operating in photon-counting mode or a MCP-enhanced CCD detector (MgF_2 window with S20 photocathode).

The electron beam was operated in three modes. A short pulsed mode with 5 ns beam pulses and 10 kHz repetition rate was used for time resolved measurements. This technique is described in detail in [3]. Direct current (dc) and long pulsed (200 ns beam pulses, 100–10 000 Hz rate) modes were used to measure photon fluxes (photons per second). For the dc operation mode the photon flux was directly measured with a counter. In the long pulsed mode the counter was gated during 500 ns starting at the beginning of each beam pulse.

3 Results and discussions

3.1 Time evolution analysis

According to the literature [6,10], the temporal evolution of emission intensity from nitrogen following a short excitation pulse shows a monoexponential decay for all bands of the SPS. The monoexponential character of the decay suggests that either any population flow to the vibrational levels of the C $^3\Pi_u$ state during the decay phase is negligible or the species which supply this population have effective lifetimes similar to the one of the emitting state. However, our experiments show that when nitrogen is excited with ∼5 ns (FWHM, see Fig. 2 in Ref. [3] for the pulse shape) electron beam pulses, there is a noticeable difference in the time evolution of emission from vibrational levels 0 and 1 in the early phase of the decay. This effect is best visible at a gas pressure of 100 hPa, as shown in Figure 1. Note that for $v' = 1$ the decay becomes exponential already ∼5 ns after the end of a 5 ns excitation pulse, while the $v' = 0$ decay shows an exponential behaviour only after about 25 ns. The fact is confirmed by varying the starting point of an exponential fit and noting the time interval after which the fitting gives consistent effective decay times. This difference in the decay behaviour might be considered as a direct indication of the fact that the vibrational levels of the C $^3\Pi_u$ state (at least $v' = 0$) are populated not only by direct electron impact excitation. An alternative explanation of this decay behaviour could be given: due to cooling of electrons after the end of an electron beam pulse the vibrational level 0, which has lower excitation energy, can be excited longer than the level 1. However, this explanation is not very likely.

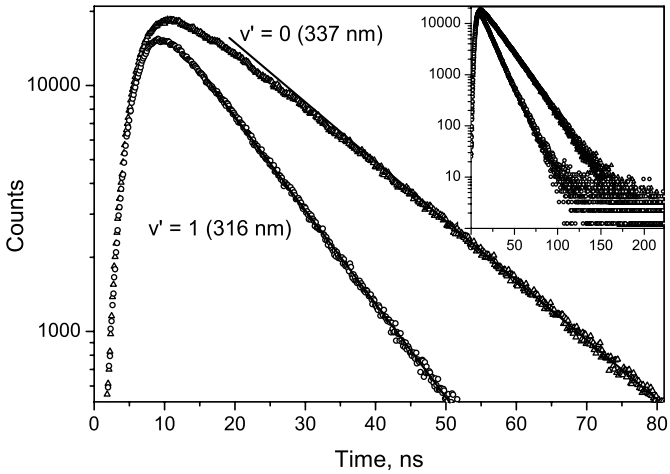

Fig. 1. Time evolution of the light emission from 100 hPa N_2. The insert shows the full time range, while the main graph demonstrates the nonexponential character of the $v = 0$ emission in the early phase of decay. The solid lines show extensions of exponential fits performed over the wide dynamic range shown in the insert.

The results of Slinker et al. [18] show that the slope of the electron energy distribution function in the range from 10 to 50 eV, which corresponds to the strongest excitation of the C $^3\Pi_u$ state, changes very little during the first 15 ns after the beam is switched off. This time interval covers the range from 10 to 25 ns in Figure 1. Note that the case of 'field off' from reference [18] has to be applied due to low beam currents used in our study. Weaker 380 nm ($v' = 0 \rightarrow v'' = 1$) and 375.5 nm ($v' = 1 \rightarrow v'' = 2$) bands show the same time evolution as the significantly stronger 337 and 316 nm bands, confirming the absence of any detector saturation effects in Figure 1.

Following the procedures described in [3] and acquiring better statistics, the following radiative decay rates r_i and quenching rate constants Q_i were obtained for vibrational level $i = 0$ and 1 at a gas temperature of 294 K: $r_0 = (2.66 \pm 0.1) \times 10^7\ s^{-1}$, $Q_0 = (1.27 \pm 0.04) \times 10^{-11}\ cm^3\ s^{-1}$ (measured from $0 \rightarrow 0$ transition) and $r_1 = (2.60 \pm 0.15) \times 10^7\ s^{-1}$, $Q_1 = (2.68 \pm 0.08) \times 10^{-11}\ cm^3\ s^{-1}$ ($1 \rightarrow 0$ transition). The uncertainties include statistical and fitting errors as well as uncertainties of the pressure measurements and data acquisition. The discrepancy with our previously published data [3] results from a correction in the calibration of the time-to-amplitude module which decreased the previously recorded effective decay times by 4%.

3.2 Flux ratio analysis

More information can be obtained by studying time-integrated photon fluxes of the SPS bands as a function of nitrogen pressure. In this study, we have recorded the photon fluxes (wavelength-integrated over the whole band) using dc and pulsed (200 ns) electron beam excitation for a broad range of nitrogen pressures. An example of spectra around 377 nm is given in Figure 2. This figure shows

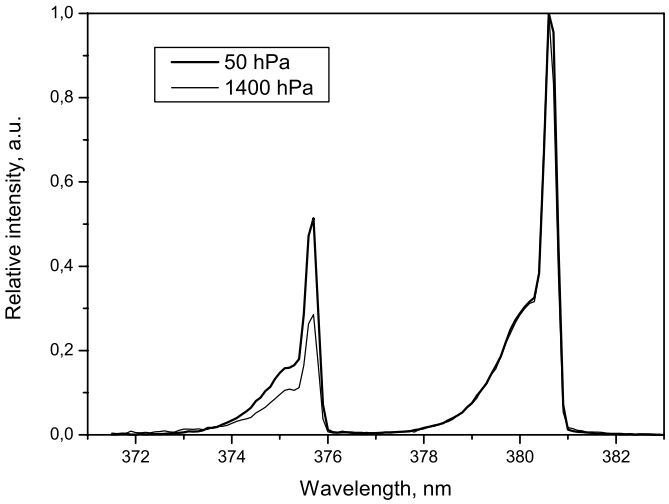

Fig. 2. Photon fluxes (scaled) recorded at two nitrogen pressures of 50 and 1400 hPa.

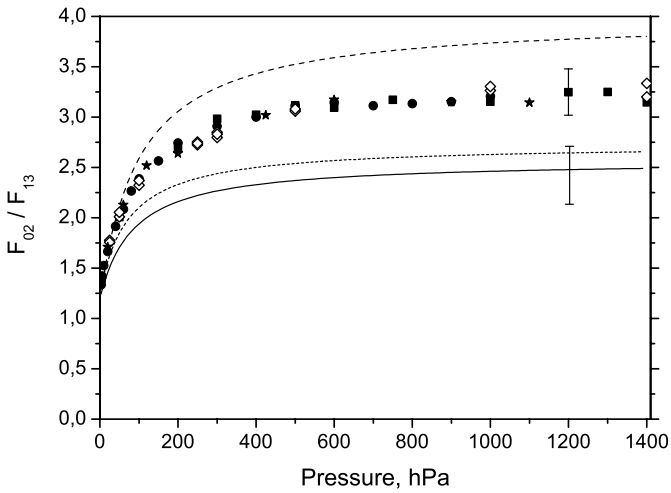

Fig. 3. Ratio of photon fluxes recorded from the $0 \rightarrow 2$ and $1 \rightarrow 3$ transitions for 5 μA dc current (full dots), 10 μA dc current (full squares) and 200 ns pulsed operation (open diamonds). The results of calculations according to the "no extra excitation" model are shown as a solid line for the present work's quenching data and as a short-dashed line for the quenching data from [6]. The long-dashed line is calculated according to the vibrational relaxation model [5]. Star symbols show the synthetic F_{02}/F_{13} flux ratio calculated from F_{01}/F_{12} data (see text).

the $v' = 0 \rightarrow v'' = 2$ (∼380.6 nm) and $v' = 1 \rightarrow v'' = 3$ (∼375.6 nm) transitions for 50 and 1400 hPa. The fluxes are scaled so that the $0 \rightarrow 2$ band amplitude is matched at both pressures. Note that the fluxes change with pressure due to two factors. Firstly, the depopulation rate of vibrational levels depends on pressure and secondly, the observation efficiency of the light emitting volume is also affected by the pressure [19]. Since the variation of the latter factor with pressure is not known with sufficient precision, we have limited our analysis to the ratio of photon fluxes of SPS bands. In this approach the observation efficiency is the same for both fluxes and can be excluded from the analysis.

The ratio of photon fluxes F_{02}/F_{13} for the bands at 380.6 and 375.6 nm is shown in Figure 3. The fluxes were derived by integrating the photon count rate over the whole wavelength range of each band. The experimental data include the flux ratios for dc electron beams of 5 and 10 μA as well as for long pulsed (200 ns) operation. Two conclusions can be drawn from the fact that the experimental data are identical for all these conditions. Firstly, it shows that processes which involve collisions of electrons with excited nitrogen have a negligible effect on the population distribution of the vibrational levels since there is no dependence on electron beam current which defines the electron density in the target gas. Secondly, there is no significant redistribution of the population of the vibrational levels after ∼300 ns from the end of an electron beam pulse (gated interval of the detection in the pulsed mode is 500 ns: 200 ns during the beam pulse and 300 ns in the afterglow).

Since significant accumulation of molecular and atomic species (metastable nitrogen molecules, atomic nitrogen, molecular nitrogen ions, etc.) might occur during dc operation or pulsed modes with high repetition rate, a series of measurements has been performed to show that the combined effect of all these species to the excitation of the C $^3\Pi_u$ state is negligible at our experimental conditions.

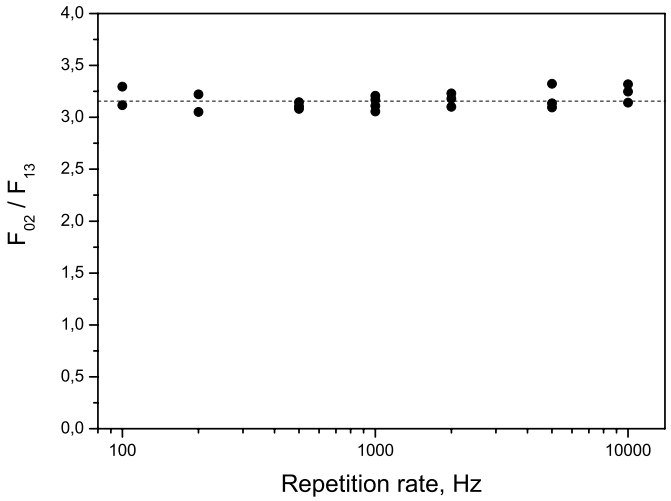

Fig. 4. Ratio of photon fluxes recorded from the $0 \rightarrow 2$ and $1 \rightarrow 3$ transitions using 200 ns pulsed excitation with different repetition rates.

As shown in Figure 4, the ratio of photon fluxes F_{02}/F_{13} at 1000 hPa does not change with the repetition rate from 10 000 down to 100 Hz. Note that the 0.01 s time interval between the electron beam pulses is comparable with the time (<0.1 s) required for the gas circulation to completely replace the gas in the excitation region.

The data presented in Figure 3 can be compared with predictions made by two models. In the first model we

assume that the only excitation mechanism populating the C $^3\Pi_u$ state is direct electron excitation. In this case the wavelength-integrated photon flux from $v' = i \rightarrow v'' = j$ transition is

$$F_{ij}(P) = g(P)\frac{r_i}{k_i(P)}\frac{A_{ij}}{A_i}E_i = g(P)\frac{A_{ij}}{k_i(P)}E_i \qquad (1)$$

where P is the nitrogen pressure, $g(P)$ is the geometrical factor which describes the variation of the detection efficiency with pressure, r_i is the radiative decay rate of the state i, $k_i(P)$ is the total decay rate of state i (radiative decay plus collisional depopulations), A_{ij} is the Einstein coefficient for the $i \rightarrow j$ transition, A_i is the sum of the Einstein coefficients for all possible transitions from the state i ($A_i = r_i$), and E_i is the excitation rate of vibrational level i due to electron impact excitation (i.e. the total population of level i created per unit time in the gas).

E_i is proportional to the excitation efficiency of state i. At high pressures E_i is independent of pressure since the total energy deposited by the electron beam in the gas is independent of gas pressure. The proportionality between the deposited energy and emission intensity has been discussed in reference [19]. At low pressures (<100 hPa for our experimental setup) a part of the electrons can reach the cell walls and E_i will be reduced by a certain factor from the value at high pressures. However, this effect is irrelevant for the analysis of photon flux ratios since the reduction factor is the same for all vibrational levels.

In order to calculate the ratio of excitation efficiencies for individual vibrational levels of the C $^3\Pi_u$ state, the following convolution has to be performed for each vibrational level i:

$$E_i \propto \int_0^\infty \sigma_i(\varepsilon)\sqrt{\varepsilon}f(\varepsilon)d\varepsilon \qquad (2)$$

where ε is the electron energy, $\sigma_i(\varepsilon)$ is the excitation cross section and $f(\varepsilon)$ is the electron energy distribution function (EEDF). Detailed data for individual vibrational levels of the C $^3\Pi_u$ state are published only for emission cross sections derived from observations of the SPS emission at very low gas pressures when the contribution of collisional cascades is negligible (see Refs. [20–23] or a review [24]). As it is shown below, relative emission cross sections for individual vibrational levels show good agreement with relative excitation cross section available for several energies. Since only relative data are required for the analysis performed in this paper, this fact validates the usage of emission cross sections. In the present work, we use the energy dependence of the emission cross section for the three lowest vibrational levels given in reference [20]. We extrapolated the cross sections to higher energies (ε from 17.5 to 100 eV) using the $\varepsilon^{-2.2}$ dependence as given in reference [25]. Note that Fons et al. [22] give an $\varepsilon^{-2.3}$ dependence while Shemansky et al. [23] suggest an ε^{-2} approximation. However, all these approximations do not affect much the results of the convolution (<1%). The resulting curves are shown in Figure 5 (solid lines) together with

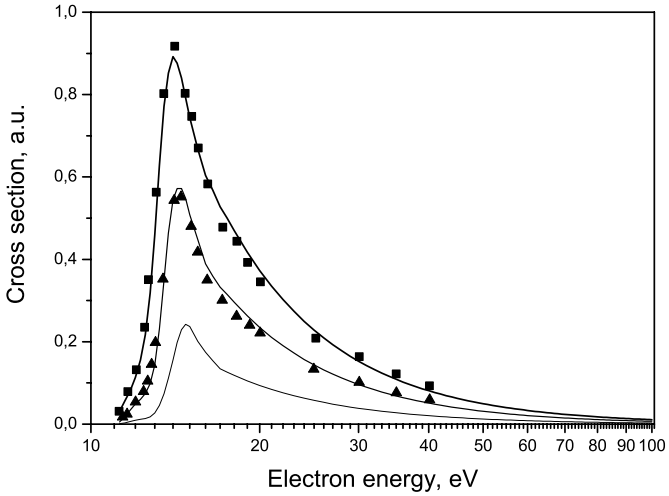

Fig. 5. Relative excitation cross sections (straight lines) used here in the excitation efficiency calculations. The shape of the excitation functions for $v' = 0$, 1 are compared with the results from reference [23] which are shown as squares ($v' = 0$) and triangles ($v' = 1$).

the data from Shemansky et al. [23] (dots). The amplitudes of the cross sections from reference [23] were scaled keeping the ratio between the curves as given in Table 3 of reference [23]. These two data sets show a good agreement in the shape of the excitation functions, as well as in the results of the convolution (<3.5% difference). Also, the relative emission cross sections from reference [20] which we use here, show a very good agreement with relative excitation cross sections measured in electron energy loss experiments [21] as well as with relative emission cross sections measured by other groups (see Tab. 2).

The EEDF for electron beam excited gases has been calculated for high pressure and high current experiments [18,26] as well as for low pressure conditions [27]. These EEDFs, in contrast to typical EEDFs for electrical discharges, show a rather slow reduction with energy in the range of 10 to 100 eV, as shown in Figure 6. Convoluting the cross sections obtained above with the EEDFs from references [18,27] using equation (2) we obtain the relative excitation efficiencies for $v' = 0$, 1 and 2 shown in Table 2. The difference in the results using two different EEDFs (2.5% for $v' = 1$ and 5% for $v' = 2$) demonstrates that the exact shape of the EEDF is not critical for electron beam excitation.

Using the ratio of 1:0.59 for the excitation efficiencies of the vibrational levels 0 and 1 and taking the A_{ij} values from reference [11] we calculated the pressure dependence of the flux ratios. The solid and short-dashed lines in Figure 3 show the results of the calculation using the quenching rate constants from the present work and from reference [6], respectively. The error bars for the solid line show the uncertainty which results from two main factors: the 8% experimental uncertainty of the quenching and radiative decay rate data as well as the uncertainty in the excitation efficiency ratio (+7% and −9%), which is estimated

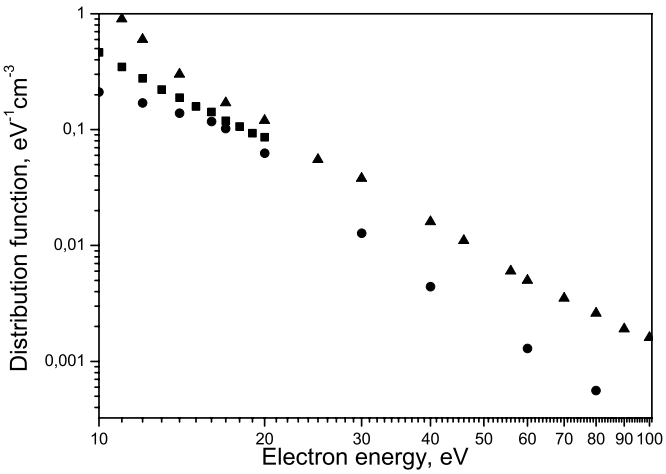

Fig. 6. Scaled electron energy distribution functions from reference [18] (triangles), reference [26] (squares) and calculated from the flux data given in reference [27] (dots).

as the maximum deviations of the data of Table 2 from the results of reference [20] used in our calculations. Note that at very low pressures, where collisional effects are greatly reduced, the solid line nearly matches the experimental flux ratios, supporting the calculated excitation efficiency ratio. As a cross-check of the experimental procedure and the validity of A_{ij} values from reference [11], a synthetic flux ratio F_{02}/F_{13} was calculated using experimental data for the F_{01}/F_{12} ratio and taking the corresponding A_{ij} values. The result is shown in Figure 3 with star-shaped dots.

Comparison of the experimental data with the predictions of the model where no extra excitation mechanisms have been applied (solid line in Fig. 3) shows a considerable (with respect to the error bars) difference between the experimental flux ratios and the ratios predicted by the model. Therefore we conclude that this difference between the calculations and the experiments suggests the presence of an excitation mechanism which populates C $^3\Pi_u$ vibrational levels in addition to direct electron impact excitation. This mechanism could be vibrational relaxation within the C $^3\Pi_u$ state or collisional quenching of upper electronic states of N_2, which were directly excited by the electron beam.

The ratios of emission fluxes from levels 0 and 1 were also measured in 80% N_2–20% O_2 and 80% N_2–20% H_2 mixtures at 1000 hPa total pressure. Oxygen and hydrogen were added since these gases strongly quench the C $^3\Pi_u$ state of nitrogen [6,9], therefore one can expect strong suppression of any additional excitation channel due to the competition with collisional quenching by the admixture. For example, $v' = 1$ level quenching would be increased by a factor of four compared with pure nitrogen, thus decreasing the population supplied to the $v' = 0$ in vibrational relaxation by the same factor. The experimental ratio of the fluxes was found to be 1.53 ± 0.06 for the oxygen mixture and 1.39 ± 0.08 for the hydrogen mixture. A model similar to the one described above with the addition of quenching by oxygen or hydrogen gives the values of 1.45 and 1.50 for the mixture with oxygen, using the quenching rates by oxygen reported in references [6,9], respectively. A value of 1.37 was calculated for the hydrogen containing mixture using the quenching rates by hydrogen from reference [6]. Here we have assumed that there is no significant modification of the EEDF in the range of 10 to 100 eV in the presence of oxygen or hydrogen. The uncertainties of the theoretical results (approximately 10%) are defined mainly by the uncertainties of the oxygen (or hydrogen) quenching rates. The results show that in both mixtures the model gives values very close to the experimental ones, thus supporting the existence of additional excitation channels in pure nitrogen.

The flux ratio of vibrational levels 0 and 1 in pure nitrogen can also be calculated using the results of Dilecce et al. [5] who provide vibrational relaxation and quenching rate constants of the five lowest vibrational levels of the C $^3\Pi_u$ state. Extending the approach which is used in the first model by taking into account the population supplied by the upper vibrational levels we obtain the pressure dependence for the flux ratio as shown by the long-dashed line in Figure 3. Here, the population supplied by vibrational level i to level j per second (S_{ij}) is calculated (in iterations starting at level 2) as

$$S_{ij} = \frac{V_{ij}P}{k_i(P)}\left(E_i + \sum_{n>i} S_{ni}\right) \qquad (3)$$

where V_{ij} is the rate constant for vibrational relaxation from level i to j. The ratios of the excitation efficiencies were taken as 1:0.59:0.22 (averaged convolution data, see Tab. 2). The vibrational levels $v' = 3$ and 4 give a practically negligible contribution to the populations of the lower states.

This model gives flux ratios higher than observed in our experiment. However, the ∼10% uncertainty in the relaxation and quenching rate constants given in reference [5] results in more than 15% overall uncertainty in the flux ratios, thus producing an overlap of the error bars for the calculated and the experimental data. We would like to note that the value for the total collisional quenching rate for $v' = 1$ reported in reference [5] is somewhat too high (compare with other Q_1 values in Tab. 1). A reduction of this value would result in a better agreement with our experimental flux data.

3.3 Comparison with published data

To our best knowledge, only one paper [10] has been published where the pressure dependence of ratios of SPS band intensities from dense nitrogen has been analysed in experiments with excitation by energetic particles. In this paper, Calo and Axtmann studied the ratio of total intensities from the vibrational levels 0 and 1 multiplied with the effective decay rate of level 0. In our terms this product corresponds to

$$Y(P) \equiv \frac{F_{0m}(P)}{F_{1n}(P)}\frac{A_{1n}}{A_{0m}}\frac{k_0(P)}{r_0}. \qquad (4)$$

Table 1. Radiative rates r (in 10^7 s^{-1}) and collisional quenching rate constants Q (in 10^{-11} cm^3s^{-1}) of the C^3 Π_u state of nitrogen for the vibrational level 0 and 1.

r_0	r_1	Q_0	Q_1	Method and reference
2.66 ± 0.1	2.60 ± 0.15	1.27 ± 0.04	2.68 ± 0.08	This work
2.77 ± 0.05	2.67 ± 0.02	1.14 ± 0.12	3.14 ± 0.21	OODR-LIF [5]
2.38 ± 0.11	2.44 ± 0.18	1.3 ± 0.2	2.9 ± 0.3	Discharge [6]
2.45		0.71		1 MeV e^- [7]
2.38 ± 0.12	2.44 ± 0.12	1.09 ± 0.11	2.53 ± 0.25	2 MeV protons [8]
3.3 ± 0.2	2.7 ± 0.2	1.13 ± 0.06	2.74 ± 0.18	2.8 MeV α [9]
2.37 ± 0.08	2.25 ± 0.07	1.31 ± 0.05	2.6 ± 0.7	Fission fragments [10]
2.69	2.61			Calculations [11]
2.67 ± 0.07				Review [12]

Table 2. Top: literature data on relative excitation cross section of the N_2 C $^3\Pi_u$ state taken at different electron energies or at the cross section maxima. Bottom: relative excitation rates calculated using two different electron energy distribution functions (see text).

Reference	σ_i/σ_0 at	$v'=0$	$v'=1$	$v'=2$	$v'=3$	$v'=4$
[20]	14 eV	1	0.610	0.174		
	17 eV	1	0.630	0.255		
	maxima		1	0.64	0.27	
[21]	17.5 eV	1	0.620	0.230	0.066	
	20 eV	1	0.666	0.280	0.085	
[22]	maxima	1	0.70	0.26	0.081	0.041
[23]	14 eV	1	0.566	0.152	0.57	0.13
	20 eV	1	0.639	0.174	0.062	0.015
Convolution, EEDF from [18]	maxima	1	0.581	0.215		
Convolution, EEDF from [27]	maxima	1	0.596	0.226		

Experimental results presented in [10] show that the pressure dependence of Y is not linear (see the graph of corrected luminosity ratio vs. pressure in Ref. [10]). By comparing their formula (14) and (17), Calo and Axtmann concluded that the nonlinearity rules out population of the C $^3\Pi_u$ state via collisional quenching of the states E $^3\Sigma_g^+$ C′ $^3\Pi_u$ and D $^3\Sigma_u^+$ and claimed the existence of a strong vibrational relaxation within the C $^3\Pi_u$ state. Rate constants for vibrational relaxation between the levels 1 and 0, and, as a rough estimation, between 2 and 1 were obtained by fitting their experimental data [10].

However, $Y(P)$ calculated from our measurements shows a linear dependence on pressure. Moreover, there is an inconsistency in reference [10]. Equation (14) of reference [10], which gives $Y(P)$ and is used to fit the experimental data, is correct. However, a plot of Y according to this equation shows practically a linear dependence on pressure when the values from Table I of reference [10] are inserted, in contrast to the fitting curve shown in Figure 4 of reference [10]. Note that the figure captions of Figures 4 and 5 in reference [10] appear to be swapped. The inconsistency mentioned above leads to the conclusion that the vibrational rate constants given by Calo and Axtmann cannot be considered reliable. Also, additional population channels due to quenching of energetically higher lying electronic states cannot be excluded.

4 Concluding remarks

This study confirms the presence of collisional excitation mechanisms populating $v' = 0$, 1 levels of the N_2 C $^3\Pi_u$ state in addition to electron impact excitation for 12 keV electron beam excitation conditions. Such mechanisms could be vibrational relaxation within the C $^3\Pi_u$ state or collisional quenching of upper electronic states of molecular nitrogen. It is shown that for the conditions of this study there is no C $^3\Pi_u$ excitation due to any species accumulated in dc or pulsed modes with high repetition rates (e.g. metastable nitrogen molecules or atomic nitrogen). State-selective excitation techniques are required to reliably investigate the particular role of the higher lying electronic states in the C $^3\Pi_u$ state excitation.

References

1. D.M. Phillips, J. Phys. D **8**, 507 (1975)
2. M. Šimek, S. DeBenedictis, G. Dilecce, V. Babicky, M. Člupek, P. Šunka, J. Phys. D **35**, 1981 (2002)
3. A. Morozov, R. Krücken, J. Wieser, A. Ulrich, Eur. Phys. J. D **33**, 207 (2005)
4. M. Nagano, K. Kobayakawa, N. Sakaki, K. Ando, Astropart. Phys. **20**, 293 (2003)

5. G. Dilecce, P.F. Ambrico, S. DeBenedictis, Chem. Phys. Lett. **431**, 241 (2006)
6. S.V. Pancheshnyi, S.M. Starikovskaia, A.Yu. Starikovskii, Chem. Phys. **262**, 349 (2000)
7. T.W. Carr, S. Dondes, J. Phys. Chem. **81**, 2225 (1977).
8. C.H. Chen, M.G. Payne, G.S. Hurst, J.P. Judish, J. Chem. Phys. **65**, 3863 (1976)
9. P. Millet, Y. Salamero, H. Brunet, J. Galy, D. Blanc, J.L. Teyssier, J. Chem. Phys. **58**, 5839 (1973)
10. J.M. Calo, R.C. Axtmann, J. Chem. Phys. **54**, 1332 (1971)
11. F.R. Gilmore, R.R. Laher, P.J. Espy, J. Chem. Ref. Data **21**, 1005 (1992)
12. P. Erman, Phys. Rev. A **48**, R3421 (1993)
13. T.G. Finn, J.F.M. Aarts, J.P. Doering, J. Chem. Phys. **56**, 5632 (1972)
14. L. Kurzweg, G.T. Egbert, D.J. Burns, Phys. Rev. A **7**, 1966 (1973)
15. F. Blanco, F. Arqueros, Phys. Lett. A **345**, 355 (2005)
16. P. Colin et al., Astropart. Phys. **27**, 317 (2007)
17. M. Ave et al., Astropart. Phys. **28**, 41 (2007)
18. S.P. Slinker, A.W. Ali, R.D. Taylor, J. Appl. Phys. **67**, 679 (1990)
19. A. Morozov, R. Krücken, A. Ulrich, J. Wieser, J. Appl. Phys. **100**, 093305 (2006)
20. M. Zubek, J. Phys. B **27**, 573 (1994)
21. M. Zubek, G.C. King, J. Phys. B **27**, 2613 (1994)
22. J.T. Fons, R.S. Schappe, C.C. Lin, Phys. Rev. A **53**, 2239 (1996)
23. D.E. Shemansky, J.M. Ajello, I. Kanik, Astroph. J. **452**, 472 (1995)
24. Y. Itikawa, J. Phys. Chem. Ref. Data **35**, 31 (2006)
25. M. Imami, W.L. Borst, J. Chem. Phys. **61**, 1115 (1974)
26. K. S. Klopovsky, A.V. Mukhovatova, A.M. Popov, N.A. Popov, O.B. Popovicheva, T.V. Rakhimova, J. Phys. D **27**, 1399 (1994)
27. D.R. Suhre, J.T. Verdeyen, J. Appl. Phys. **47**, 4484 (1976)